23rd Australasian Fluid Mechanics Conference – 23AFMC
Sydney, Australia
4-8 December 2022
Paper No: AFMC2022-011

Unsteady air entrainment in dam break waves and bores: theoretical considerations

Hubert Chanson [1]

[1] School of Civil Engineering, The University of Queensland, Brisbane, QLD 4072, Australia

* Email: h.chanson@uq.edu.au

Abstract

Flash flood waves have been responsible for numerous losses of life, with related extreme events encompassing dam break, tsunami, landslide dam failures and glacier lake outburst floods (GLOF). Visual observations demonstrated a strong aeration of the leading, although this aspect remains mostly unquantified. For a dam break wave in a dry chute, limited void fraction experimental data showed a time-evolution of the vertical profiles from a convex to a concave shape in the roller region. In the present study, the equation of conservation of mass for air in the air-water flow gives a novel theoretical solution of the vertical profiles of void fraction within the front. The new analytical model was successfully validated with unsteady air-water flow measurements in dam break over dry bed and breaking bore over a wet bed. The results deliver some seminal insights into the unsteady interfacial processes in a dam break wave, including potential effects in terms of scale effects.

1. Introduction

Flood waves resulting from flash floods have been responsible for numerous damage and losses of life (Jonkman 2005). Related extreme events encompass dam break wave following a rapid dam failure (e.g. Malpasset dam), tsunami bores overtopping coastal defences (e.g. 2004 Boxing Day tsunami, 2011 Tohoku tsunami), landslide dam failures (e.g. Grenoble AD 1219) and glacier lake outburst floods (GLOF) (Lauber 1997, Galay 1987, Mori et al. 2012). In all cases, visual observations demonstrated a strong aeration of the advancing front, but this aspect remains mostly unknown and unquantified. For a dam break wave in a dry chute, limited void fraction experimental data showed a time-evolution of the vertical profiles from a convex to a concave shape for $0 < z/Z_{90} < 1$, with z the vertical elevation and Z_{90} the characteristic elevation where the void fraction equals $C = 0.90$ (Chanson 2004, 2005). As in dam break waves, a similar temporal evolution of the vertical profile of void fraction was recently reported in a breaking bore roller (Leng and Chanson 2019a,b).

In open channel flows, free-surface aeration is caused by turbulent fluctuations acting next to the air-water free surface (Ervine and Falvey 1997, Chanson 2009). Through this interface, air is continuously trapped and released in an uncontrolled fashion. Interfacial aeration involves both entrainment of air bubbles and formation of water droplets (Rao and Kobus 1974, Wood 1991). The exact location of the interface becomes undetermined, and there are continuous exchanges of air-water and of momentum between water and atmosphere. The air-water mix consists of water surrounding air bubbles (bubbly flow: $C < 30\%$), air surrounding water droplets (spray: $C > 70\%$) and an intermediate flow structure for $0.3 < C < 0.7$, with C the void fraction (Chanson 1997, Felder and Chanson 2016).

Considering a small control volume within a dam break wave, the equation of conservation of mass for air in the air-water flow gives a theoretical solution of the vertical profiles of void fraction within the front. The new analytical model is successfully validated with unsteady air-water flow measurements in dam break over dry bed and breaking bore over a wet bed. The results deliver some seminal insights into the unsteady interfacial processes in the dam break wave front.

(A)

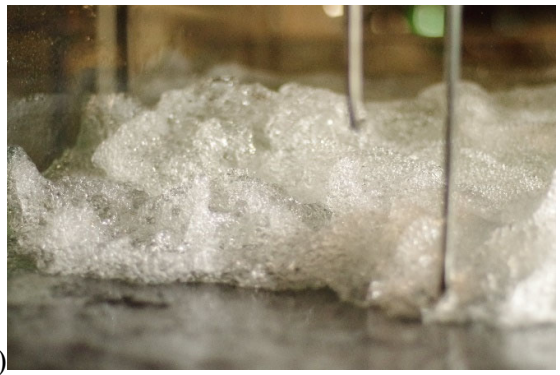

(B)

(C)

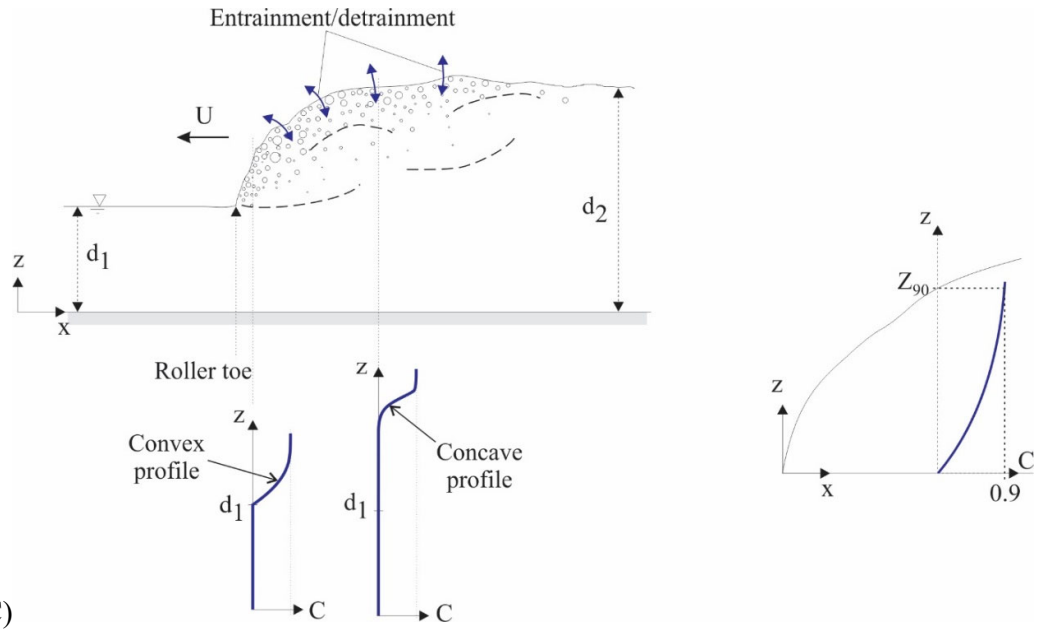

Figure 1. Definition sketch of self-aeration in an advancing breaking bore roller. (A-B) High-shutter-speed photographs of travelling bore (Fr_1 = 2.4, Re = 2×10^5), (A) looking downstream at incoming bore and (B) side view (bore direction from right to left). (C) Side view and schematic of simplified roller aeration (Right)

2. Analytical solution for dam break wave and breaking bore roller

In an advancing breaking roller, the initial flow ahead of the roller is typically non-aerated. With the passage of the bore front, strong interfacial aeration and de-aeration take place through the upper surface of the roller, with surface breaking and uncontrolled air exchanges (Figure 1). In first approximation, the turbulent diffusion of air into the roller must counterbalance the detrainment

induced by buoyancy effects. For a small control volume within the roller, the equation of conservation of mass for air in the air-water flow gives:

$$\frac{\partial}{\partial z}\left(D_t \times \frac{\partial C}{\partial z} \right) = \frac{\partial}{\partial z}\left(C \times u_r \right), \quad (1)$$

with z is the vertical direction (Figure 1C), D_t is the turbulent diffusivity of air, C is the void fraction and u_r is the rise velocity of a bubble in an air-water mixture.

The ratio of bubble rise velocity in air-water mixture to rise velocity in clear-water may be expressed as:

$$\frac{{u_r}^2}{{[u_r]_{CW}}^2} = \frac{[C_d]_{CW} \times \rho_w}{C_d \times \rho} \times (1 - C), \quad (2)$$

irrespective of the bubble shape, with $[C_d]_{CW}$ the drag coefficient of a bubble rising in clear-water, ρ the relevant fluid density for drag coefficient calculation, ρ_w the water density and the subscript CW corresponding to clear-water flow properties (Appendix I).

Replacing into Equation (1), the equation of conservation of mass for air in the air-water flow becomes in dimensionless form:

$$D' \times \frac{\partial C}{\partial z'} = C \times \sqrt{1 - C} \times \sqrt{\frac{[C_d]_{CW} \times \rho_w}{C_d \times \rho}}, \quad (3)$$

with:

$$D' = \frac{D_t}{(Z_{90} - d_1) \times [u_r]_{CW}}, \quad (4)$$

$z' = (z-d_1)/(Z_{90}-d_1)$, and d_1 the initial depth (Figure 1C). Equation (3) applies to the aerated roller region, i.e. $0 < z' < 1$.

Assuming in first approximation $[C_d]_{CW} \times \rho_w/(C_d \times \rho) \approx 1$, and that the air bubble diffusivity D' is zero for C = 0 and C = 1, and follows:

$$D' = \frac{1}{N} \times \sqrt{1 - C} \times \left(\frac{C}{0.9} \right)^{1/N}, \quad \text{with } N > 0 \quad (5)$$

the integration of the equation of mass for air (Equation (3)) yields the void fraction profile:

$$C = 0.9 \times z'^{N}, \quad \text{with } N > 0 \quad (6)$$

where the exponent N is related to the depth-averaged void fraction C_{mean} in the roller (i.e. $d_1 < z < Z_{90}$):

$$C_{mean} = \frac{1}{Z_{90} - d_1} \times \int_{z=d_1}^{Z_{90}} C \times dz = \frac{0.9}{N+1}, \quad (7)$$

2.1 Discussion

For N < 1. the vertical distribution of void fraction presents a convex profile for $0 < (z-d_1)/(Z_{90}-d_1) < 1$. The case N= 0.5 corresponds to the analytical model first developed by Chanson and Toombes (2001) and applied successfully to transition flows on stepped spillways. For N > 1, a concave shape is observed (Figure 2). Typical distributions of C and D' are presented in Figure 2.

The present development is based upon a number of basic assumptions (Chanson 2021). First, the flow is assumed to be quasi-steady and the analysis is performed in the system of references in translation with the bore roller toe. Although Equations (6) and (7) do not reflect a time dependency, both the depth-averaged void fraction C_{mean} and exponent 1/N implicitly vary with time. Second, the bore roller is assumed to be fully-developed and its shape is quasi-steady, i.e. it does not change with time. Third, self-aeration is predominantly an interfacial process with uncontrolled exchanges of air through the roller surface, assuming no or negligible air entrapment at

the roller toe. This would consistent with the CFD numerical and physical data of Leng et al. (2018) and Leng and Chanson (2019b) respectively. Fourth, the turbulent diffusion of air is predominantly a vertical exchange, i.e. the turbulent diffusion of air in the vertical direction counterbalances exactly the buoyancy effect.

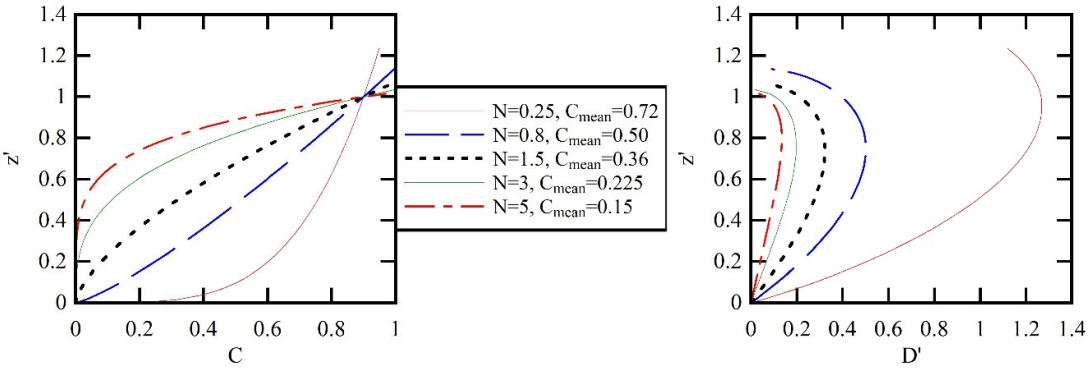

Figure 2. Vertical dimensionless distributions of void fraction C (Equation (6)) and dimensionless diffusivity for air D' (Equation (5)) in an advancing breaking bore roller. Same legend for both graphs.

3. Applications

3.1 Dam break wave on dry bed

Dam break wave physical experiments were carried out in a 24 m long 0.5 m long channel, initially dry, equipped with a stepped invert (Chanson 2004). Void fraction measurements were conducted with an array of phase-detection probes. The void fraction experimental data recorded at step edges showed a time-evolution of the vertical profiles from a convex profile at the leading edge to a concave shape, as illustrated in Figure 3. The figure caption lists the boundary and flow conditions, including the channel breadth B.

Basically, the convex vertical distribution of void fraction at the leading edge corresponded to very large depth-averaged void fraction. Further behind, the profile evolved into a concave shape, with significantly lesser depth-averaged void fraction (Figure 3).

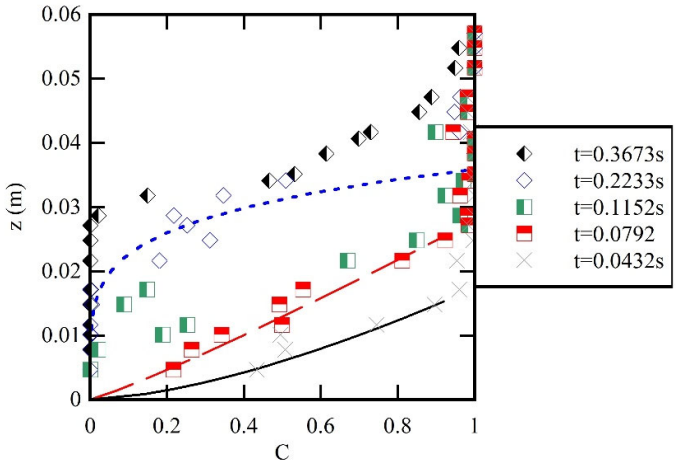

Figure 3. Void fraction distributions in dam break wave front on dry bed. Data: Chanson (2004), Run TL5, Step 16, x' = 1.0 m, Q(t=0+) = 0.075 m^3/s, B = 0.5 m, U = 2.3 m/s, t = time since the leading edge passage. Comparison with Equation (6) (solid, dashed and dotted lines).

3.2 Breaking bore roller

Detailed unsteady air-water flow measurements were conducted in a breaking bore with a Froude number Fr_1 = 2.4 and a Reynolds number Re = 1.86×10^5 (Shi et al. 2021) (Figs. 1A & 1B). The experiments were undertaken in a 19 m long, 0.7 m wide and 0.5 m deep tilting flume, previously used by Leng and Chanson (2019a). The breaking bore was generated by the rapid closure of a Tainter gate located at the downstream end of the flume. The bore propagated upstream with a celerity U, positive upstream. Herein, the coordinate x is the direction of the initially steady flow, and y and z are the transverse and vertical coordinates respectively. The air-water measurements were recorded with double-tip phase detection probes (Ø = 0.25 mm) sampled at 100 Hz. The experiments were repeated 100 times and the data ensemble were analysed.

Typical ensemble-averaged instantaneous void fraction <C> are presented in Figure 4. Note the different time steps between Figures 3 and 4. This resulted from the faster dam break wave celerity. In Figure 4, the data are further compared with Equation (6). The result showed a good agreement between data and analytical solution. For completeness, the data of Leng and Chanson (2019a, 2019b) presented similarly a good agreement with Equation (6) with a lower Froude number.

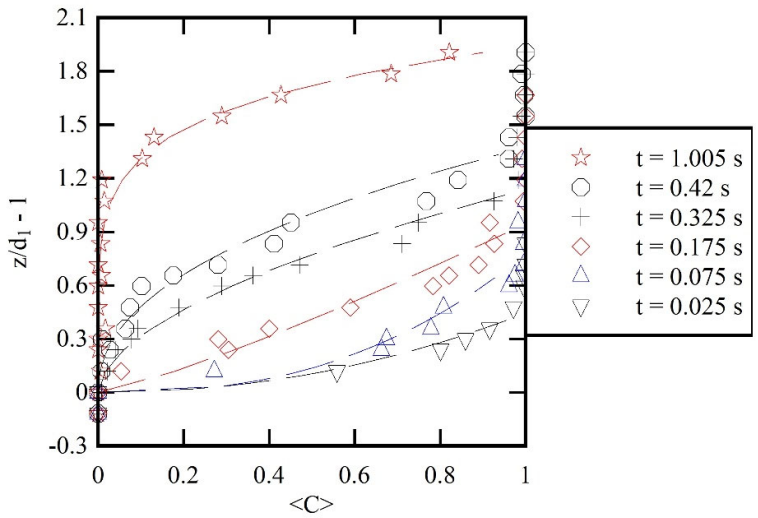

Figure 4. Vertical distributions of instantaneous ensemble-averaged void fraction in a breaking bore roller. Data: Shi et al. (2021), d_1 = 0.084 mm, B = 0.70 m, U = 0.504 m/s, Δd = 0.162 m, Fr_1 = 2.4, t = time since the leading edge passage of bore roller. Comparison with Equation (6) (Dashed lines).

4. Discussion

In a breaking bore roller and dam break wave, the temporal evolution of the instantaneous depth-averaged void fraction C_{mean} in the roller showed a distinctive shape (Figure 5a). For $t \times (g/\Delta d)^{1/2} < 0.6$, the mean void fraction in the bore's leading edge was nearly constant and about 0.6, with Δd being the roller height. For larger times $t \times (g/\Delta d)^{1/2} > 0.6$, an exponential decay in mean void fraction was observed. Typical data are presented in Figure 5a, with a semilogarithmic presentation. Importantly, the void fraction distributions showed some surface aeration limited to the upper roller region. With increasing roller thickness with increasing time, the results implied a very rapid relative de-aeration of the roller region across the upper flow region. Quantitatively, the findings were similar for the dam break wave data, as illustrated in Figure 5a.

The depth-averaged dimensionless diffusivity $(D')_{mean}$ data presented typical values between 0.08 and 0.11 irrespective of time, except near the tail end of the roller (Figure 5b). The breaking bore results were quantitatively close to dam break wave data, despite the physical differences between the two processes. The dimensionless diffusivity observations may further be compared to detailed

air-water flow measurements in self-aerated chute flows, hydraulic jumps and plunging jets (Figure 6). Figure 6 presents dimensionless diffusivity data $D_t/(U\times(Z_{90}-d_1))$ as functions of the Reynolds number $\rho_w\times U\times(Z_{90}-d_1)/\mu_w$, following a presentation first proposed by Chanson (1997, pp. 131-132 & 222). The present data fitted the general trend showing a decaying dimensionless diffusivity with increasing Reynolds number, irrespective of the typology of self-aeration flow motion, across a wide range of Reynolds number, i.e. $10^4 < Re < 3\times10^7$ (Figure 6). The result confirmed earlier findings (Chanson 1995, Zhang and Chanson 2017) that small-size physical laboratories of steady and unsteady self-aerated flows are unlikely to characterise accurately the air bubble diffusion process, and implicitly the competition between air bubble entrainment and momentum exchanges.

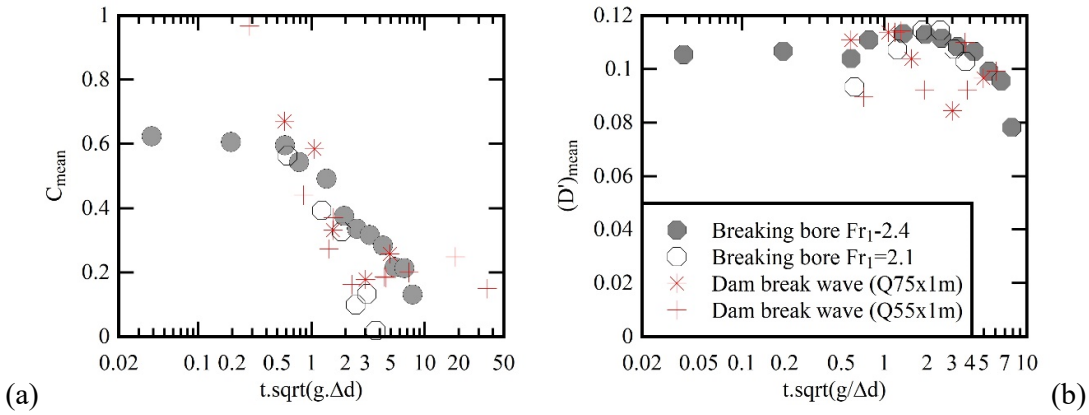

Figure 5. Temporal evolution of (a) instantaneous depth-averaged roller void fraction C_{mean} and (b) depth-averaged turbulent diffusivity $(D')_{mean}$: comparison between break bore and dam break wave data. Breaking bore data: Leng and Chanson (2019b), Shi et al. (2021). Dam break wave data: Chanson (2004).

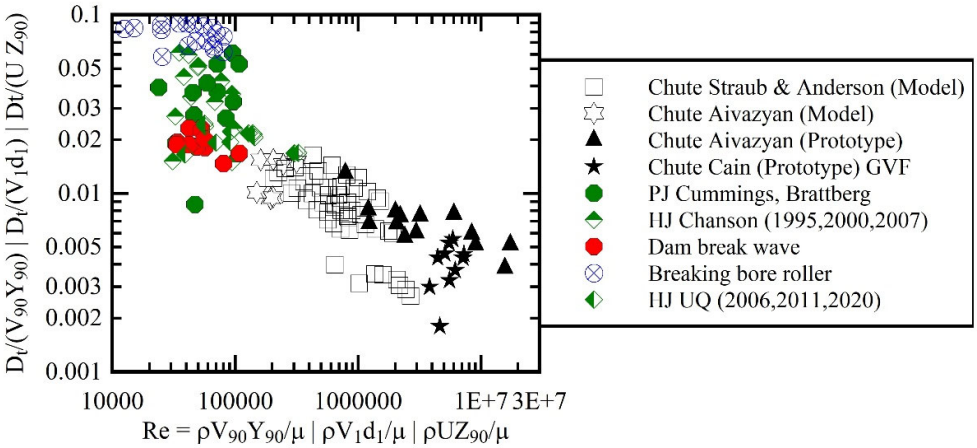

Figure 6. Dimensionless depth-averaged turbulent diffusivity as a function of the Reynolds number in steady and unsteady self-aerated flows. Comparison with experimental observations in self-aerated smooth chute flows, hydraulic jumps (HJ) and vertical supported jets (PJ).

5. Conclusion

A new theoretical model of advective diffusion of air in self-aerated flows was developed for transient breaking bore and dam break wave. The time evolution of vertical void fraction profiles showed a change from a convex shape to a concave distribution in the breaking roller with increasing time. The new model compared favourably with both breaking bore and dam break wave

data. The results implied a very strong flow aeration at the leading edge, with a rapid de-aeration of the flow, while the dimensionless diffusivity remained mostly constant independently of time.

The present data analysis yielded a general trend implying a decreasing dimensionless diffusivity with increasing Reynolds number, irrespective of the self-aeration type for $10^4 < Re < 3\times10^7$. The finding hinted strongly that small-size laboratory facilities cannot accurately characterise the air bubble diffusion process of self-aerated flows in large-scale prototype. The result is most important in practice, with direct implications in hydraulic modelling, including numerical studies validated with small-size laboratory data sets.

Appendix I. Bubble rise velocity in self-aerated flow

The buoyant force on an air bubble in a fluid is the difference between the vertical components of the pressure force on its underside and on its upper side. For an air bubble subjected to a hydrostatic pressure gradient in an air-water self-aerated flow, the buoyant force equals the weight of displaced liquid (i.e. air-water mixture). Considering the terminal bubble rise velocity $[u_r]_{CW}$ in a clear-water chute flow, analytical expressions can be derived for any bubble shape (Clift et al. 1978, Comolet 1979). Because of interfacial processes, little information is known on the bubble drag coefficient in an air-water mixture. In bubbly flows, the interactions between bubbles are important factors affecting the entire drag process, beyond the change in surrounding fluid density. Some works suggested that the ratio $C_d/[C_d]_{CW}$ increases monotonically with increasing void fraction (Lockett and Kirkpatrick 1975, Roghair et al. 2012).

Acknowledgments

The author acknowledges helpful discussions with Dr Rui Shi (The University of Queensland) and Dr Davide Wüthrich (TU Delft).

References

Chanson, H. (1995). "Air Bubble Diffusion in Supercritical Open Channel Flow." *Proc. 12th Australasian Fluid Mechanics Conference AFMC*, Sydney, Australia, R.W. Bilger Ed., Vol. 2, pp. 707-710

Chanson, H. (1997). "*Air Bubble Entrainment in Free-Surface Turbulent Shear Flows*." Academic Press, London, UK, 401 pages.

Chanson, H. (2004). "Unsteady Air-Water Flow Measurements in Sudden Open Channel Flows." *Experiments in Fluids*, Vol. 37, No. 6, pp. 899-909 (DOI: 10.1007/s00348-004-0882-3).

Chanson, H. (2005). "Air-Water and Momentum Exchanges in Unsteady Surging Waters: an Experimental Study." *Experimental Thermal and Fluid Science*, Vol. 30, No. 1, pp. 37-4747 (DOI: 10.1016/j.expthermflusci.2005.03.017).

Chanson, H. (2009). "Turbulent Air-water Flows in Hydraulic Structures: Dynamic Similarity and Scale Effects." *Environmental Fluid Mechanics*, Vol. 9, No. 2, pp. 125-142 (DOI: 10.1007/s10652-008-9078-3).

Chanson, H. (2021). "Advective diffusion of air in dam break wave and breaking bore." in "Air-water characteristics of a breaking bore roller Part II: Air-water flow properties." *Hydraulic Model Report No. CH118/20*, School of Civil Engineering, The University of Queensland, Brisbane, Australia, by Shi, R., Wüthrich, D., and Chanson H., pp. B-1–B-15.

Chanson, H., and Toombes, L. (2001). "Strong Interactions between Free-Surface Aeration and Turbulence down a Staircase Channel." *Proceedings 14th Australasian Fluid Mechanics Conference*, Adelaide, Australia, pp. 841-844

Clift, R., Grace, J.R., and Weber, M.E. (1978). "*Bubbles, Drops, and Particles*." Academic Press, San Diego, USA, 380 pages.

Comolet, R. (1979). "Sur le Mouvement d'une bulle de gaz dans un liquide." ('Gas Bubble Motion in a Liquid Medium.') *Jl La Houille Blanche*, No. 1, pp. 31-42 (in French).

Ervine, D.A., and Falvey, H.T. (1987). "Behaviour of Turbulent Water Jets in the Atmosphere and in Plunge Pools." *Proceedings of the Institution Civil Engineers, London, Part 2*, Mar. 1987, 83, pp. 295-314.

Felder, S., and Chanson, H. (2016). "Air–water flow characteristics in high-velocity free-surface flows with 50% void fraction." *International Journal of Multiphase Flow*, Vol. 85, pp. 186-195(DOI: 10.1016/j.ijmultiphaseflow.2016.06.004)

Galay, V. (1987). "*Erosion and Sedimentation in the Nepal Himalaya. An Assessment of River Processes*." CIDA, ICIMOD, IDRC & Kefford Press, Singapore.

Jonkman, S.N. (2005). "Global perspectives on loss of human life caused by floods." *Natural Hazards*, Vol. 34, pp.151–175.

Lauber, G. (1997). "Experimente zur Talsperrenbruchwelle im glatten geneigten Rechteckkanal." ('Dam Break Wave Experiments in Rectangular Channels.') *Ph.D. thesis*, VAW-ETH, Zürich, Switzerland (in German).

Leng, X., and Chanson, H. (2019a). "Two-phase Flow Measurements of an Unsteady Breaking Bore." *Experiments in Fluids*, Vol. 60, No. 3, Paper 42, 15 pages & 2 video movies (DOI: 10.1007/s00348-019-2689-2).

Leng, X., and Chanson, H. (2019b). "Air-Water Interaction and Characteristics in Breaking Bores." *International Journal of Multiphase Flow*, Vol. 120, Paper 103101, 17 pages (DOI: 10.1016/j.ijmultiphaseflow.2019.103101).

Leng, X., Simon, B., Khezri, N., Lubin, P., and Chanson, H. (2018). "CFD Modelling of Tidal Bores: Development and Validation Challenges." *Coastal Engineering Journal*, Vol. 60, No. 4, pp. 423-436 (DOI: 10.1080/21664250.2018.1498211)

Lockett, M. J., and Kirkpatrick, R. D. (1975). "Ideal bubbly flow and actual flow in bubble columns." *Transactions of the Institution of Chemical Engineers*, Vol. 53, pp. 267–273.

Mori, N., and Takahashi, T. (2012). "Nationwide Post Event Survey and Analysis of the 2011 Tohoku Earthquale Tsunami." *Coastal Engineering Journal*, Vo. 54, No. 1, Paper 1250001, 27 pages.

Rao, N.S.L., and Kobus, H.E. (1974). "*Characteristics of Self-Aerated Free-Surface Flows*." Water and Waste Water/Current Research and Practice, Vol. 10, Eric Schmidt Verlag, Berlin, Germany, 224 pages.

Roghair, I., Lau, Y.M., Deen, N.G., Slagter, H.M., Baltussen, M.W., Van Sint Annaland, M., Kuipers, J.A.M. (2011). "On the drag force of bubbles in bubble swarms at intermediate and high Reynolds numbers." Chemical Engineering Science, Vol. 66, pp. 3204–3211 (DOI: 10.1016/j.ces.2011.02.030).

Shi, R., Wüthrich, D. and Chanson, H. (2021). "Air-water characteristics of a breaking bore roller Part II: Air-water flow properties." *Hydraulic Model Report No. CH118/20*, School of Civil Engineering, The University of Queensland, Brisbane, Australia, 160 pages.

Wood, I.R. (1991). "*Air Entrainment in Free-Surface Flows*." IAHR Hydraulic Structures Design Manual No. 4, Hydraulic Design Considerations, Balkema Publ., Rotterdam, The Netherlands, 149 pages.

Zhang, G., and Chanson, H. (2017). "Self-aeration in the rapidly- and gradually-varying flow regions of steep smooth and stepped spillways." *Environmental Fluid Mechanics*, Vol. 17, No. 1, pp. 27-46 (DOI: 10.1007/s10652-015-9442-z).